

# Chelating the Alpha Therapy Radionuclides $^{225}\text{Ac}^{3+}$ and $^{213}\text{Bi}^{3+}$ with 18-Membered Macrocyclic Ligands MacroDipa and Py-MacroDipa

Aohan Hu, Victoria Brown, Samantha N. MacMillan, Valery Radchenko, Hua Yang, Luke Wharton, Caterina F. Ramogida, and Justin J. Wilson\*



Cite This: *Inorg. Chem.* 2022, 61, 801–806



Read Online

ACCESS |



Metrics & More



Article Recommendations



Supporting Information

**ABSTRACT:** The radionuclides  $^{225}\text{Ac}^{3+}$  and  $^{213}\text{Bi}^{3+}$  possess favorable physical properties for targeted alpha therapy (TAT), a therapeutic approach that leverages  $\alpha$  radiation to treat cancers. A chelator that effectively binds and retains these radionuclides is required for this application. The development of ligands for this purpose, however, is challenging because the large ionic radii and charge-diffuse nature of these metal ions give rise to weaker metal–ligand interactions. In this study, we evaluated two 18-membered macrocyclic chelators, macroDipa and py-macroDipa, for their ability to complex  $^{225}\text{Ac}^{3+}$  and  $^{213}\text{Bi}^{3+}$ . Their coordination chemistry with  $\text{Ac}^{3+}$  was probed computationally and with  $\text{Bi}^{3+}$  experimentally via NMR spectroscopy and X-ray crystallography. Furthermore, radiolabeling studies were conducted, revealing the efficient incorporation of both  $^{225}\text{Ac}^{3+}$  and  $^{213}\text{Bi}^{3+}$  by py-macroDipa that matches or surpasses the well-known chelators macropa and DOTA. Incubation in human serum at 37 °C showed that  $\sim 90\%$  of the  $^{225}\text{Ac}^{3+}$ –py-macroDipa complex dissociates after 1 d. The  $\text{Bi}^{3+}$ –py-macroDipa complex possesses remarkable kinetic inertness reflected by an EDTA transchelation challenge study, surpassing that of  $\text{Bi}^{3+}$ –macropa. This work establishes py-macroDipa as a valuable candidate for  $^{213}\text{Bi}^{3+}$  TAT, providing further motivation for its implementation within new radiopharmaceutical agents.

Targeted alpha therapy (TAT) is a promising therapeutic strategy that leverages  $\alpha$ -particle-emitting radionuclides to annihilate tumor cells. Compared to conventional internal radiotherapy using  $\beta$ -particle emitters, the implementation of significantly more massive  $\alpha$  particles, which deposit their energy over much shorter distances, provides key advantages. The short range of  $\alpha$  radiation can yield enhanced selectivity for targeted cancer cells, while minimizing damage to surrounding healthy cells. Moreover, the very large linear energy transfer (LET) of  $\alpha$  particles is significantly more effective in causing lethal DNA double strand breaks that kill cancer cells in a more efficacious manner compared to the lower-LET  $\beta$  particles.<sup>1–6</sup>

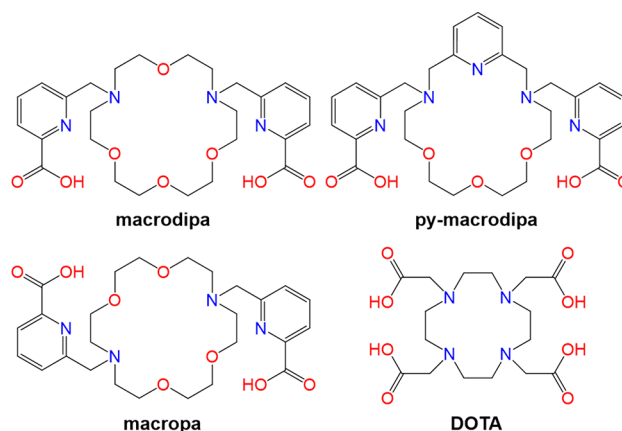
To date, over eight radionuclides have been identified as potential candidates for use in TAT based on their decay properties and production routes.<sup>7</sup> Among these nuclides,  $^{225}\text{Ac}^{3+}$  and  $^{213}\text{Bi}^{3+}$  have received considerable attention that has manifested in clinical studies.<sup>8–10</sup>  $^{225}\text{Ac}$  ( $t_{1/2} = 9.9$  d) emits four  $\alpha$  particles through its decay chain, a property that confers it with high cytotoxic potency. Its 9.9-day half-life is also well matched with the in vivo circulation timescales of macromolecular targeting vectors like antibodies.<sup>11,12</sup>  $^{213}\text{Bi}$  ( $t_{1/2} = 45.6$  min), a daughter of  $^{225}\text{Ac}^{3+}$ , emits one  $\alpha$  particle through its decay chain and can be conveniently obtained from  $^{225}\text{Ac}/^{213}\text{Bi}$  generators.<sup>13</sup> Its shorter half-life can be optimally matched to small-molecule targeting vectors, rendering it useful for different systems than those employed for  $^{225}\text{Ac}^{3+}$ .<sup>14,15</sup>

To convert these promising radionuclides into radiotherapeutic agents, a chelator that efficiently binds and stably retains them is required.<sup>16,17</sup> The development of chelators for

large metal ions like  $\text{Ac}^{3+}$  and  $\text{Bi}^{3+}$ , however, is challenging, partly because their low charge density weakens electrostatic interactions with ligand donor atoms.

We recently reported a new ligand called macroDipa<sup>18</sup> and its second-generation analogue py-macroDipa<sup>19</sup> (Chart 1). These “macroDipa-type” chelators feature a unique “dual size

**Chart 1. Structures of Chelators Discussed in This Work**



**Received:** November 24, 2021

**Published:** December 29, 2021



selectivity”, characterized by their good affinities for both the large and small rare-earth metal ions ( $\text{Ln}^{3+}$ ). This unusual selectivity profile arises from a significant conformational toggle that occurs when they form complexes with  $\text{Ln}^{3+}$  ions of different sizes. Large  $\text{Ln}^{3+}$  form 10-coordinate, nearly  $C_2$ -symmetric complexes (Conformation A), whereas an 8-coordinate, asymmetric complex arises for small  $\text{Ln}^{3+}$  (Conformation B).<sup>18,19</sup> We have further demonstrated that this property makes py-macrodipa a valuable candidate for nuclear medicine applications with both  $^{135}\text{La}^{3+}$  and  $^{44}\text{Sc}^{3+}$ ,  $\text{Ln}^{3+}$  radiometal ions with the largest and smallest ionic radii within this series.<sup>19</sup>

Based on this successful application of macrodipa and py-macrodipa for the  $\text{Ln}^{3+}$  ions, we sought to evaluate these ligands with biomedically relevant ions beyond the  $\text{Ln}^{3+}$  series, namely  $\text{Ac}^{3+}$  and  $\text{Bi}^{3+}$ . The potentials of both chelators for TAT applications using their radioisotopes  $^{225}\text{Ac}^{3+}$  and  $^{213}\text{Bi}^{3+}$  were determined and benchmarked to those of the well-known chelators macropa and DOTA (Chart 1), which have established precedence for nuclear medicine applications with these radiometals.<sup>20–23</sup>

We assessed the coordination chemistry of these ligands with stable  $\text{Bi}^{3+}$ . The  $^1\text{H}$  and  $^{13}\text{C}\{^1\text{H}\}$  NMR spectra of their  $\text{Bi}^{3+}$  complexes ( $\text{Bi}^{3+}$ -macrodipa and  $\text{Bi}^{3+}$ -py-macrodipa) were acquired in  $\text{D}_2\text{O}$  (Figures 1 and S1–S4). These spectra

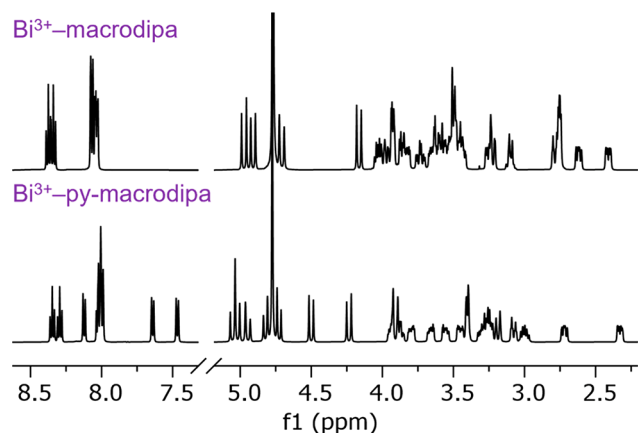


**Figure 1.**  $^1\text{H}$  NMR spectra of  $\text{Bi}^{3+}$ -macrodipa and  $\text{Bi}^{3+}$ -py-macrodipa (500 MHz,  $\text{D}_2\text{O}$ , pD 5, 25 °C).

reveal the presence of a single, well-resolved species that lacks symmetry for both complexes. Thus,  $\text{Bi}^{3+}$ -macrodipa and  $\text{Bi}^{3+}$ -py-macrodipa most likely attain the asymmetric Conformation B, which is the preferred binding mode of these ligands for small  $\text{Ln}^{3+}$  (Figures S5–S6).

As further validation, we characterized  $\text{Bi}^{3+}$ -macrodipa and  $\text{Bi}^{3+}$ -py-macrodipa by X-ray crystallography (Figure 2). The crystal structures of these complexes confirm that they attain the asymmetric Conformation B, consistent with our observations from NMR spectroscopy. Like their NMR spectra, these  $\text{Bi}^{3+}$  structures are comparable to those of the small  $\text{Ln}^{3+}$  analogues,  $\text{Lu}^{3+}$ -macrodipa and  $\text{Sc}^{3+}$ -py-macrodipa, with respect to the orientation of the picolinate donors and the lack of full engagement of all six macrocycle donor atoms.<sup>18,19</sup> A key difference between these  $\text{Ln}^{3+}$  and  $\text{Bi}^{3+}$  structures, however, is the absence of a coordinated water molecule in the latter. This void is most likely a consequence of the stereochemical activity<sup>24,25</sup> of the  $\text{Bi}^{3+}$   $6s^2$  lone pair. These observations that  $\text{Bi}^{3+}$ -macrodipa and  $\text{Bi}^{3+}$ -py-macro-

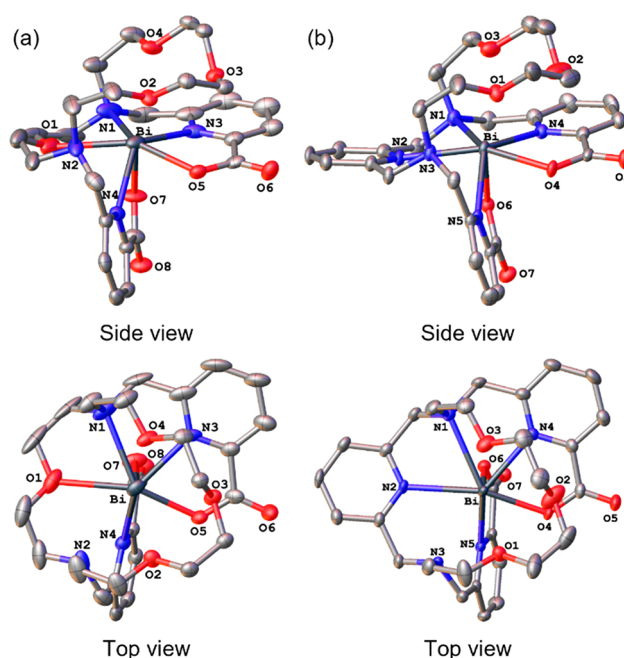


**Figure 2.** Crystal structures of (a)  $[\text{Bi}(\text{macrodipa})]^+$  and (b)  $[\text{Bi}(\text{py-macrodipa})]^+$ . Thermal ellipsoids are drawn at the 50% probability level. Solvent and counterions are omitted for clarity.

dipa attain the asymmetric Conformation B rather than the symmetric Conformation A is somewhat surprising based on the similar ionic radii of  $\text{Bi}^{3+}$  and  $\text{La}^{3+}$ ,<sup>26,27</sup> a representative large  $\text{Ln}^{3+}$ . This result suggests that the stereochemical activity of the  $6s^2$  lone pair plays a pronounced role in mediating the preferred conformations of these  $\text{Bi}^{3+}$  complexes.

Experimental characterization of  $\text{Ac}^{3+}$  complexes is challenging due to the high radioactivity and extremely limited availability of its longest-lived isotope  $^{227}\text{Ac}$  ( $t_{1/2} = 21.8$  y).<sup>28</sup> Thus, we instead probed the structures of  $\text{Ac}^{3+}$ -macrodipa and  $\text{Ac}^{3+}$ -py-macrodipa computationally using density functional theory (DFT) with *Gaussian 16*.<sup>29</sup> The hybrid TPSSH functional,<sup>30</sup> which has been validated for studying  $\text{Ac}^{3+}$  chemistry,<sup>31,32</sup> was adopted. A large-core relativistic effective core potential (LCRECP) and the associated basis set was assigned to the  $\text{Ac}^{3+}$  center,<sup>33–35</sup> whereas the 6-31G(d,p) basis set<sup>36,37</sup> was applied to all other lighter atoms. Aqueous solvation effects were accounted for with the SMD solvation model.<sup>38</sup>

Because the ionic radii and coordination chemistry of  $\text{Ac}^{3+}$  and  $\text{La}^{3+}$  are similar,<sup>28</sup> we optimized  $\text{Ac}^{3+}$ -macrodipa and  $\text{Ac}^{3+}$ -py-macrodipa starting from the geometries of the corresponding  $\text{La}^{3+}$  complexes, which attain the symmetric Conformation A.<sup>18,19</sup> Within these structures (Figure 3), the Ac–O interatomic distances are 2.45–2.48 Å for negatively charged O and 2.70–2.79 Å for neutral O, whereas the Ac–N interactions range from 2.76–2.92 Å. These calculated distances are close to experimentally measured Ac–O and Ac–N interatomic distances.<sup>39–43</sup> Additionally, we optimized both complexes in Conformation B. Consistent with our expectations, Conformation B is energetically disfavored for both complexes (Table S2).

Having established the coordination chemistry of these ligands, we next carried out radiolabeling studies to evaluate their potential value for  $^{225}\text{Ac}^{3+}$  and  $^{213}\text{Bi}^{3+}$  TAT in comparison to the state-of-the-art chelators macropa and DOTA. These

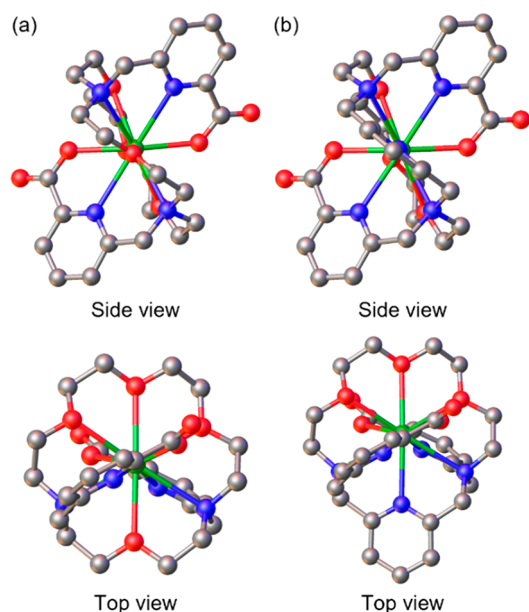


**Figure 3.** DFT-optimized structures of (a)  $[\text{Ac}(\text{macrodipa})]^+$  and (b)  $[\text{Ac}(\text{py-macrodipa})]^+$ . Hydrogen atoms are omitted for clarity. Green: Ac. Gray: C. Blue: N. Red: O.

radionuclides were produced and purified according to previously described protocols.<sup>44–46</sup>

Different concentrations of macrodipa, py-macrodipa, macropa, and DOTA were combined with pH 5.5–6 buffered solutions containing either 20–40 or 30–300 kBq of  $^{225}\text{Ac}^{3+}$  and  $^{213}\text{Bi}^{3+}$  at ambient or elevated temperature, and the radiochemical yields (RCYs) were determined by radio-TLC. The concentration-dependent RCYs for these four chelators are summarized in Figure 4. For both radionuclides, py-macrodipa is able to achieve significantly higher RCYs than its analogue macrodipa and the conventional chelator DOTA, which also required high temperatures for radiolabeling. RCYs of approximately 75% and 65% are obtained when using low py-macrodipa concentrations of  $10^{-6}$  M and  $10^{-8}$  M for  $^{225}\text{Ac}^{3+}$  and  $^{213}\text{Bi}^{3+}$ , respectively. With respect to  $^{225}\text{Ac}^{3+}$  chelation, py-macrodipa was slightly less effective than macropa, but was better at radiolabeling  $^{213}\text{Bi}^{3+}$ . We also performed  $^{225}\text{Ac}^{3+}$  radiolabeling with macrodipa and py-macrodipa at pH 7 (Table S3). Under this condition, both chelators were able to access greater RCYs, but still failed to surpass macropa. Overall, these studies show that py-macrodipa effectively radiolabels both  $^{225}\text{Ac}^{3+}$  and  $^{213}\text{Bi}^{3+}$  under mild conditions.

We next assessed the kinetic inertness of  $^{225}\text{Ac}^{3+}$ –py-macrodipa by incubating it in human serum at 37 °C (Table S5). These studies show that  $^{225}\text{Ac}^{3+}$ –py-macrodipa is fairly labile, as ~90% of the complex dissociated after 1 d. By contrast,  $^{225}\text{Ac}^{3+}$ –macropa remained 98% intact in human serum after 5 d. This excellent kinetic inertness is consistent with a previously reported serum challenge on  $^{225}\text{Ac}^{3+}$ –macropa.<sup>20</sup> Hence, despite the efficient radiolabeling properties of py-macrodipa, it is not an optimal candidate for TAT applications with  $^{225}\text{Ac}^{3+}$ .

Because  $^{213}\text{Bi}^{3+}$  decays quickly ( $t_{1/2} = 45.6$  min), probing the  $^{213}\text{Bi}^{3+}$  complex kinetic inertness by this serum challenge assay is impractical. Instead, we performed a transchelation challenge assay<sup>19–21,47–49</sup> on the macrodipa, py-macrodipa, and macropa

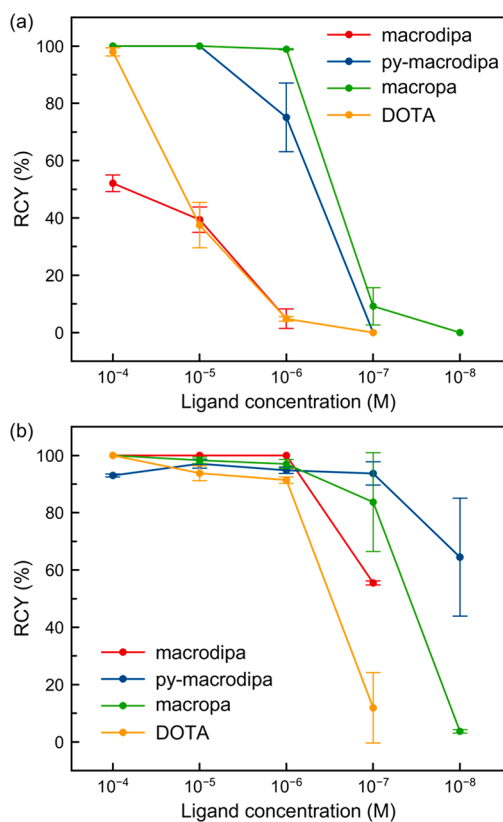


**Figure 4.** Radiochemical yields at different ligand concentrations. (a) RCYs of  $^{225}\text{Ac}^{3+}$  radiolabeling (25 °C for py-macrodipa, macropa, 40 °C for macrodipa, and 80 °C for DOTA; pH 5.5–6; 60 min reaction time). (b) RCYs of  $^{213}\text{Bi}^{3+}$  labeling (25 °C for macrodipa, py-macrodipa, macropa and 95 °C for DOTA; pH 5.5–6; 6–8 min reaction time). Error bars represent the standard deviations. The  $^{213}\text{Bi}^{3+}$  data with macropa and DOTA was taken from ref 21.

complexes with stable  $\text{Bi}^{3+}$ . The transchelation reactions of these  $\text{Bi}^{3+}$  complexes were monitored by UV–Vis spectroscopy in the presence of a 10-fold excess EDTA, a ligand with high affinity for  $\text{Bi}^{3+}$ ,<sup>50,51</sup> at pH 5.0 and 25 °C. Under this condition, the  $\text{Bi}^{3+}$  ion is transchelated by EDTA, following pseudo-first-order kinetics. The resulting half-lives ( $t_{1/2}$ ) for this transchelation process, a comparative measure of complex kinetic inertness, are shown in Table 1.  $\text{Bi}^{3+}$ –macrodipa is kinetically

**Table 1.** Half-Lives of  $\text{Bi}^{3+}$  Complexes when Challenged with 10 Equivalents of EDTA<sup>a</sup>

	$t_{1/2}$
$\text{Bi}^{3+}$ –macrodipa	$9.2 \pm 0.1$ min
$\text{Bi}^{3+}$ –py-macrodipa	$13.2 \pm 1.2$ d
$\text{Bi}^{3+}$ –macropa	$2.2 \pm 0.2$ d

<sup>a</sup> $[\text{BiL}] = 100 \mu\text{M}$ , pH 5.0, 25 °C.

labile to this transchelation challenge. The kinetic inertness of  $\text{Bi}^{3+}$ –py-macrodipa is remarkably enhanced, as reflected by a  $t_{1/2}$  of 13 d. Moreover, its inertness is greater than that of  $\text{Bi}^{3+}$ –macropa, indicating that py-macrodipa is a promising candidate for TAT applications with  $^{213}\text{Bi}^{3+}$ .

In summary, we evaluated the viability of macrodipa and py-macrodipa as chelators for  $^{225}\text{Ac}^{3+}$  and  $^{213}\text{Bi}^{3+}$ . Their coordination chemistry with  $\text{Ac}^{3+}$  and  $\text{Bi}^{3+}$  were characterized computationally and experimentally, respectively. Our radio-



labeling studies revealed that py-macrodipa is highly effective at radiolabeling both radiometals, outperforming both macrodipa and DOTA. Although the lability of  $\text{Ac}^{3+}$ -py-macrodipa precludes its use with  $^{225}\text{Ac}^{3+}$  in nuclear medicine, the efficient formation and high stability of  $\text{Bi}^{3+}$ -py-macrodipa, which surpasses  $\text{Bi}^{3+}$ -macropa, suggests that this ligand is a valuable candidate for  $^{213}\text{Bi}^{3+}$  chelation. These results highlight that py-macrodipa joins other promising candidates for  $^{213}\text{Bi}^{3+}$  chelation that have arisen in recent years.<sup>21,52–60</sup> Ongoing work is directed toward the synthesis of a bifunctional analogue of py-macrodipa to apply this chelator in TAT, as well as the development of “macrodipa-type” chelators with enhanced  $\text{Ac}^{3+}$  complex stabilities.

## ■ ASSOCIATED CONTENT

### SI Supporting Information

The Supporting Information is available free of charge at <https://pubs.acs.org/doi/10.1021/acs.inorgchem.1c03670>.

Experimental procedures and supplementary data (PDF)

Geometry outputs for DFT-optimized structures (ZIP)

### Accession Codes

CCDC 2124116–2124117 contain the supplementary crystallographic data for this paper. These data can be obtained free of charge via [www.ccdc.cam.ac.uk/data\\_request/cif](http://www.ccdc.cam.ac.uk/data_request/cif), or by emailing [data\\_request@ccdc.cam.ac.uk](mailto:data_request@ccdc.cam.ac.uk), or by contacting The Cambridge Crystallographic Data Centre, 12 Union Road, Cambridge CB2 1EZ, UK; fax: +44 1223 336033.

## ■ AUTHOR INFORMATION

### Corresponding Author

Justin J. Wilson – Department of Chemistry and Chemical Biology, Cornell University, Ithaca, New York 14853, United States; [orcid.org/0000-0002-4086-7982](https://orcid.org/0000-0002-4086-7982);  
Email: [jjw275@cornell.edu](mailto:jjw275@cornell.edu)

### Authors

Aohan Hu – Department of Chemistry and Chemical Biology, Cornell University, Ithaca, New York 14853, United States; [orcid.org/0000-0002-9720-3159](https://orcid.org/0000-0002-9720-3159)

Victoria Brown – Department of Chemistry, Simon Fraser University, Burnaby, British Columbia V5A 1S6, Canada; [orcid.org/0000-0002-0216-3538](https://orcid.org/0000-0002-0216-3538)

Samantha N. MacMillan – Department of Chemistry and Chemical Biology, Cornell University, Ithaca, New York 14853, United States; [orcid.org/0000-0001-6516-1823](https://orcid.org/0000-0001-6516-1823)

Valery Radchenko – Life Sciences Division, TRIUMF, Vancouver, British Columbia V6T 2A3, Canada; Department of Chemistry, University of British Columbia, Vancouver, British Columbia V6T 1Z1, Canada

Hua Yang – Life Sciences Division, TRIUMF, Vancouver, British Columbia V6T 2A3, Canada; Department of Chemistry, Simon Fraser University, Burnaby, British Columbia V5A 1S6, Canada; [orcid.org/0000-0003-1833-9515](https://orcid.org/0000-0003-1833-9515)

Luke Wharton – Department of Chemistry, University of British Columbia, Vancouver, British Columbia V6T 1Z1, Canada; Life Sciences Division, TRIUMF, Vancouver, British Columbia V6T 2A3, Canada; [orcid.org/0000-0002-0636-8741](https://orcid.org/0000-0002-0636-8741)

Caterina F. Ramogida – Department of Chemistry, Simon Fraser University, Burnaby, British Columbia V5A 1S6, Canada; Life Sciences Division, TRIUMF, Vancouver, British

Columbia V6T 2A3, Canada; [orcid.org/0000-0003-4815-2647](https://orcid.org/0000-0003-4815-2647)

Complete contact information is available at:

<https://pubs.acs.org/doi/10.1021/acs.inorgchem.1c03670>

## Notes

The authors declare the following competing financial interest(s): J. J. Wilson and A. Hu have filed a provisional patent on the py-macrodipa chelator for nuclear medicine applications.

## ■ ACKNOWLEDGMENTS

This research was supported by the National Institutes of Biomedical Imaging and Bioengineering of the National Institutes of Health under Award Numbers R21EB027282 and R01EB029259, as well as the Research Corporation for Science Advancement through a Cottrell Research Scholar Award to J.J.W. This research made use of the NMR Facility at Cornell University, which was supported, in part, by the U.S. National Science Foundation under award number CHE-1531632. TRIUMF receives funding via a contribution agreement with the Natural Research Council of Canada. The authors acknowledge the TRIUMF actinium-production team for their work to produce and isolate  $^{225}\text{Ac}$  from the 500 MeV Isotope Production Facility. V.B. was funded by a Natural Sciences and Engineering Research Council (NSERC) Canada Graduate Scholarship—Masters (CGS-M).

## ■ REFERENCES

- (1) Brechbiel, M. W. Targeted  $\alpha$ -Therapy: Past, Present, Future? *Dalton Trans.* **2007**, 4918–4928.
- (2) Kim, Y.-S.; Brechbiel, M. W. An Overview of Targeted Alpha Therapy. *Tumor Biol.* **2012**, *33*, 573–590.
- (3) Seidl, C. Radioimmunotherapy with  $\alpha$ -Particle-Emitting Radionuclides. *Immunotherapy* **2014**, *6*, 431–458.
- (4) Guerra Liberal, F. D. C.; O’Sullivan, J. M.; McMahan, S. J.; Prise, K. M. Targeted Alpha Therapy: Current Clinical Applications. *Cancer Biother. Radiopharm.* **2020**, *35*, 404–417.
- (5) Radchenko, V.; Morgenstern, A.; Jalilian, A. R.; Ramogida, C. F.; Cutler, C.; Duchemin, C.; Hoehr, C.; Haddad, F.; Bruchertseifer, F.; Gausemel, H.; Yang, H.; Osso, J. A.; Washiyama, K.; Czerwinski, K.; Leufgen, K.; Pruszyński, M.; Valzdorf, O.; Causey, P.; Schaffer, P.; Perron, R.; Maxim, S.; Wilbur, D. S.; Stora, T.; Li, Y. Production and Supply of  $\alpha$ -Particle-Emitting Radionuclides for Targeted  $\alpha$ -Therapy. *J. Nucl. Med.* **2021**, *62*, 1495–1503.
- (6) Yang, H.; Wilson, J. J.; Orvig, C.; Li, Y.; Wilbur, D. S.; Ramogida, C.; Radchenko, V.; Schaffer, P. Harnessing Alpha-Emitting Radionuclides for Therapy: Radiolabeling Method Review. *J. Nucl. Med.* **2021**, DOI: 10.2967/jnumed.121.262687.
- (7) Eychenne, R.; Chérel, M.; Haddad, F.; Guérard, F.; Gestein, J.-F. Overview of the Most Promising Radionuclides for Targeted Alpha Therapy: The “Hopeful Eight”. *Pharmaceutics* **2021**, *13*, 906.
- (8) Morgenstern, A.; Apostolidis, C.; Kratochwil, C.; Satheke, M.; Krollick, L.; Bruchertseifer, F. An Overview of Targeted Alpha Therapy with  $^{225}\text{Ac}$  and  $^{213}\text{Bi}$ . *Curr. Radiopharm.* **2018**, *11*, 200–208.
- (9) Bruchertseifer, F.; Kellerbauer, A.; Malmbeck, R.; Morgenstern, A. Targeted Alpha Therapy with Bismuth-213 and Actinium-225: Meeting Future Demand. *J. Labelled Compd. Radiopharm.* **2019**, *62*, 794–802.
- (10) Morgenstern, A.; Apostolidis, C.; Bruchertseifer, F. Supply and Clinical Application of Actinium-225 and Bismuth-213. *Semin. Nucl. Med.* **2020**, *50*, 119–123.
- (11) Geerlings, M. W.; Kaspersen, F. M.; Apostolidis, C.; van der Hout, R. The Feasibility of  $^{225}\text{Ac}$  as a Source of  $\alpha$ -Particles in Radioimmunotherapy. *Nucl. Med. Commun.* **1993**, *14*, 121–125.

- (12) Thiele, N. A.; Wilson, J. J. Actinium-225 for Targeted  $\alpha$  Therapy: Coordination Chemistry and Current Chelation Approaches. *Cancer Biother. Radiopharm.* **2018**, *33*, 336–348.
- (13) Morgenstern, A.; Bruchertseifer, F.; Apostolidis, C. Bismuth-213 and Actinium-225 – Generator Performance and Evolving Therapeutic Applications of Two Generator-Derived Alpha-Emitting Radioisotopes. *Curr. Radiopharm.* **2012**, *5*, 221–227.
- (14) Hassfjell, S.; Brechbiel, M. W. The Development of the  $\alpha$ -Particle Emitting Radionuclides  $^{212}\text{Bi}$  and  $^{213}\text{Bi}$ , and Their Decay Chain Related Radionuclides, for Therapeutic Applications. *Chem. Rev.* **2001**, *101*, 2019–2036.
- (15) Ahenkorah, S.; Cassells, I.; Deroose, C. M.; Cardinaels, T.; Burgoyne, A. R.; Bormans, G.; Ooms, M.; Cleeren, F. Bismuth-213 for Targeted Radionuclide Therapy: From Atom to Bedside. *Pharmaceutics* **2021**, *13*, 599.
- (16) Price, E. W.; Orvig, C. Matching Chelators to Radiometals for Radiopharmaceuticals. *Chem. Soc. Rev.* **2014**, *43*, 260–290.
- (17) *Radiopharmaceutical Chemistry*; Lewis, J. S., Windhorst, A. D., Zeglis, B. M., Eds.; Springer Nature Switzerland AG: Cham, Switzerland, 2019.
- (18) Hu, A.; MacMillan, S. N.; Wilson, J. J. Macrocyclic Ligands with an Unprecedented Size-Selectivity Pattern for the Lanthanide Ions. *J. Am. Chem. Soc.* **2020**, *142*, 13500–13506.
- (19) Hu, A.; Aluicio-Sarduy, E.; Brown, V.; MacMillan, S. N.; Becker, K. V.; Barnhart, T. E.; Radchenko, V.; Ramogida, C. F.; Engle, J. W.; Wilson, J. J. Py-Macrodipa: A Janus Chelator Capable of Binding Medicinally Relevant Rare-Earth Radiometals of Disparate Sizes. *J. Am. Chem. Soc.* **2021**, *143*, 10429–10440.
- (20) Thiele, N. A.; Brown, V.; Kelly, J. M.; Amor-Coarasa, A.; Jermilova, U.; MacMillan, S. N.; Nikolopoulou, A.; Ponnala, S.; Ramogida, C. F.; Robertson, A. K. H.; Rodríguez-Rodríguez, C.; Schaffer, P.; Williams, C., Jr.; Babich, J. W.; Radchenko, V.; Wilson, J. J. An Eighteen-Membered Macrocyclic Ligand for Actinium-225 Targeted Alpha Therapy. *Angew. Chem., Int. Ed.* **2017**, *56*, 14712–14717.
- (21) Fiszbein, D. J.; Brown, V.; Thiele, N. A.; Woods, J. J.; Wharton, L.; MacMillan, S. N.; Radchenko, V.; Ramogida, C. F.; Wilson, J. J. Tuning the Kinetic Inertness of  $\text{Bi}^{3+}$  Complexes: The Impact of Donor Atoms on Diaza-18-Crown-6 Ligands as Chelators for  $^{213}\text{Bi}$  Targeted Alpha Therapy. *Inorg. Chem.* **2021**, *60*, 9199–9211.
- (22) McDevitt, M. R.; Ma, D.; Simon, J.; Frank, R. K.; Scheinberg, D. A. Design and Synthesis of  $^{225}\text{Ac}$  Radioimmunopharmaceuticals. *Appl. Radiat. Isot.* **2002**, *57*, 841–847.
- (23) Norenberg, J. P.; Krenning, B. J.; Konings, I. R. H. M.; Kusewitt, D. F.; Nayak, T. K.; Anderson, T. L.; de Jong, M.; Garmestani, K.; Brechbiel, M. W.; Kvols, L. K.  $^{213}\text{Bi}$ -[DOTA<sup>0</sup>, Tyr<sup>3</sup>]Octreotide Peptide Receptor Radionuclide Therapy of Pancreatic Tumors in a Preclinical Animal Model. *Clin. Cancer Res.* **2006**, *12*, 897–903.
- (24) Shimoni-Livny, L.; Glusker, J. P.; Bock, C. W. Lone Pair Functionality in Divalent Lead Compounds. *Inorg. Chem.* **1998**, *37*, 1853–1867.
- (25) Pujales-Paradela, R.; Rodríguez-Rodríguez, A.; Gayoso-Padula, A.; Brandariz, I.; Valencia, L.; Esteban-Gómez, D.; Platas-Iglesias, C. On the Consequences of the Stereochemical Activity of the  $\text{Bi(III)}$   $6s^2$  Lone Pair in Cyclen-Based Complexes. The  $[\text{Bi}(\text{DO3A})]$  Case. *Dalton Trans.* **2018**, *47*, 13830–13842.
- (26) Shannon, R. D. Revised Effective Ionic Radii and Systematic Studies of Interatomic Distances in Halides and Chalcogenides. *Acta Crystallogr., Sect. A: Found. Adv.* **1976**, *32*, 751–767.
- (27) Näslund, J.; Persson, I.; Sandström, M. Solvation of the Bismuth(III) Ion by Water, Dimethyl Sulfoxide,  $N,N'$ -Dimethylpropyleneurea, and  $N,N$ -Dimethylthioformamide. An EXAFS, Large-Angle X-ray Scattering, and Crystallographic Structural Study. *Inorg. Chem.* **2000**, *39*, 4012–4021.
- (28) Deblonde, G. J.-P.; Zavarin, M.; Kersting, A. B. The Coordination Properties and Ionic Radius of Actinium: A 120-Year-Old Enigma. *Coord. Chem. Rev.* **2021**, *446*, 214130.
- (29) Frisch, M. J.; Trucks, G. W.; Schlegel, H. B.; Scuseria, G. E.; Robb, M. A.; Cheeseman, J. R.; Scalmani, G.; Barone, V.; Petersson, G. A.; Nakatsuji, H.; Li, X.; Caricato, M.; Marenich, A. V.; Bloino, J.; Janesko, B. G.; Gomperts, R.; Mennucci, B.; Hratchian, H. P.; Ortiz, J. V.; Izmaylov, A. F.; Sonnenberg, J. L.; Williams-Young, D.; Ding, F.; Lipparini, F.; Egidi, F.; Goings, J.; Peng, B.; Petrone, A.; Henderson, T.; Ranasinghe, D.; Zakrzewski, V. G.; Gao, J.; Rega, N.; Zheng, G.; Liang, W.; Hada, M.; Ehara, M.; Toyota, K.; Fukuda, R.; Hasegawa, J.; Ishida, M.; Nakajima, T.; Honda, Y.; Kitao, O.; Nakai, H.; Vreven, T.; Throssell, K.; Montgomery, J. A., Jr.; Peralta, J. E.; Ogliaro, F.; Bearpark, M. J.; Heyd, J. J.; Brothers, E. N.; Kudin, K. N.; Staroverov, V. N.; Keith, T. A.; Kobayashi, R.; Normand, J.; Raghavachari, K.; Rendell, A. P.; Burant, J. C.; Iyengar, S. S.; Tomasi, J.; Cossi, M.; Millam, J. M.; Klene, M.; Adamo, C.; Cammi, R.; Ochterski, J. W.; Martin, R. L.; Morokuma, K.; Farkas, O.; Foresman, J. B.; Fox, D. J. *Gaussian 16*, revision C. 01; Gaussian, Inc.: Wallingford, CT, 2016.
- (30) Tao, J.; Perdew, J. P.; Staroverov, V. N.; Scuseria, G. E. Climbing the Density Functional Ladder: Nonempirical Meta-Generalized Gradient Approximation Designed for Molecules and Solids. *Phys. Rev. Lett.* **2003**, *91*, 146401.
- (31) Kovács, A. Theoretical Study of Actinide Complexes with Macropa. *ACS Omega* **2020**, *5*, 26431–26440.
- (32) Kovács, A. Theoretical Study of Actinide(III)-DOTA Complexes. *ACS Omega* **2021**, *6*, 13321–13330.
- (33) Küchle, W.; Dolg, M.; Stoll, H.; Preuss, H. Energy-Adjusted Pseudopotentials for the Actinides. Parameter Sets and Test Calculations for Thorium and Thorium Monoxide. *J. Chem. Phys.* **1994**, *100*, 7535–7542.
- (34) Cao, X.; Dolg, M.; Stoll, H. Valence Basis Sets for Relativistic Energy-Consistent Small-Core Actinide Pseudopotentials. *J. Chem. Phys.* **2003**, *118*, 487–496.
- (35) Cao, X.; Dolg, M. Segmented Contraction Scheme for Small-Core Actinide Pseudopotential Basis Sets. *J. Mol. Struct.: THEOCHEM* **2004**, *673*, 203–209.
- (36) Hehre, W. J.; Ditchfield, R.; Pople, J. A. Self-Consistent Molecular Orbital Methods. XII. Further Extensions of Gaussian-Type Basis Sets for Use in Molecular Orbital Studies of Organic Molecules. *J. Chem. Phys.* **1972**, *56*, 2257–2261.
- (37) Hariharan, P. C.; Pople, J. A. The Influence of Polarization Functions on Molecular Orbital Hydrogenation Energies. *Theor. Chim. Acta* **1973**, *28*, 213–222.
- (38) Marenich, A. V.; Cramer, C. J.; Truhlar, D. G. Universal Solvation Model Based on Solute Electron Density and on a Continuum Model of the Solvent Defined by the Bulk Dielectric Constant and Atomic Surface Tensions. *J. Phys. Chem. B* **2009**, *113*, 6378–6396.
- (39) Ferrier, M. G.; Batista, E. R.; Berg, J. M.; Birnbaum, E. R.; Cross, J. N.; Engle, J. W.; La Pierre, H. S.; Kozimor, S. A.; Lezama Pacheco, J. S.; Stein, B. W.; Stieber, S. C. E.; Wilson, J. J. Spectroscopic and Computational Investigation of Actinium Coordination Chemistry. *Nat. Commun.* **2016**, *7*, 12312.
- (40) Ferrier, M. G.; Stein, B. W.; Batista, E. R.; Berg, J. M.; Birnbaum, E. R.; Engle, J. W.; John, K. D.; Kozimor, S. A.; Lezama Pacheco, J. S.; Redman, L. N. Synthesis and Characterization of the Actinium Aquo Ion. *ACS Cent. Sci.* **2017**, *3*, 176–185.
- (41) Ferrier, M. G.; Stein, B. W.; Bone, S. E.; Cary, S. K.; Ditter, A. S.; Kozimor, S. A.; Lezama Pacheco, J. S.; Mocko, V.; Seidler, G. T. The Coordination Chemistry of  $\text{Cm}^{\text{III}}$ ,  $\text{Am}^{\text{III}}$ , and  $\text{Ac}^{\text{III}}$  in Nitrate Solutions: an Actinide  $\text{L}_3$ -Edge EXAFS Study. *Chem. Sci.* **2018**, *9*, 7078–7090.
- (42) Stein, B. W.; Morgenstern, A.; Batista, E. R.; Birnbaum, E. R.; Bone, S. E.; Cary, S. K.; Ferrier, M. G.; John, K. D.; Lezama Pacheco, J.; Kozimor, S. A.; Mocko, V.; Scott, B. L.; Yang, P. Advancing Chelation Chemistry for Actinium and Other +3 f-Elements, Am, Cm, and La. *J. Am. Chem. Soc.* **2019**, *141*, 19404–19414.
- (43) Jones, Z. R.; Livshits, M. Y.; White, F. D.; Dalodière, E.; Ferrier, M. G.; Lilley, L. M.; Knope, K. E.; Kozimor, S. A.; Mocko, V.; Scott, B. L.; Stein, B. W.; Wacker, J. N.; Woen, D. H. Advancing

Understanding of Actinide(III) (Ac, Am, Cm) Aqueous Complexation Chemistry. *Chem. Sci.* **2021**, *12*, 5638–5654.

(44) Robertson, A. K. H.; McNeil, B. L.; Yang, H.; Gendron, D.; Perron, R.; Radchenko, V.; Zeisler, S.; Causey, P.; Schaffer, P.  $^{232}\text{Th}$ -Spallation-Produced  $^{225}\text{Ac}$  with Reduced  $^{227}\text{Ac}$  Content. *Inorg. Chem.* **2020**, *59*, 12156–12165.

(45) Ma, D.; McDevitt, M. R.; Finn, R. D.; Scheinberg, D. A. Breakthrough of  $^{225}\text{Ac}$  and Its Radionuclide Daughters from an  $^{225}\text{Ac}/^{213}\text{Bi}$  Generator: Development of New Methods, Quantitative Characterization, and Implications for Clinical Use. *Appl. Radiat. Isot.* **2001**, *55*, 667–678.

(46) McDevitt, M. R.; Finn, R. D.; Sgouros, G.; Ma, D.; Scheinberg, D. A. An  $^{225}\text{Ac}/^{213}\text{Bi}$  Generator System for Therapeutic Clinical Applications: Construction and Operation. *Appl. Radiat. Isot.* **1999**, *50*, 895–904.

(47) Thiele, N. A.; Woods, J. J.; Wilson, J. J. Implementing f-Block Metal Ions in Medicine: Tuning the Size Selectivity of Expanded Macrocycles. *Inorg. Chem.* **2019**, *58*, 10483–10500.

(48) Aluicio-Sarduy, E.; Thiele, N. A.; Martin, K. E.; Vaughn, B. A.; Devaraj, J.; Olson, A. P.; Barnhart, T. E.; Wilson, J. J.; Boros, E.; Engle, J. W. Establishing Radiolanthanum Chemistry for Targeted Nuclear Medicine Applications. *Chem. - Eur. J.* **2020**, *26*, 1238–1242.

(49) Hu, A.; Keresztes, I.; MacMillan, S. N.; Yang, Y.; Ding, E.; Zipfel, W. R.; DiStasio, R. A., Jr.; Babich, J. W.; Wilson, J. J. Oxyaapa: A Picolinate-Based Ligand with Five Oxygen Donors that Strongly Chelates Lanthanides. *Inorg. Chem.* **2020**, *59*, 5116–5132.

(50) Martell, A. E.; Smith, R. M. *Critical Stability Constants*; Plenum Press: New York, 1974; Vol. 1.

(51) Ramaiah, N. A.; Tewari, G. D.; Trivedi, S. R.; Katiyar, S. S. Spectrophotometric Titration of Bismuth with EDTA. *Talanta* **1968**, *15*, 352–356.

(52) Lima, L. M. P.; Beyler, M.; Oukhatar, F.; Le Saec, P.; Faivre-Chauvet, A.; Platas-Iglesias, C.; Delgado, R.; Tripier, R.  $\text{H}_2\text{Me-do}2\text{pa}$ : An Attractive Chelator with Fast, Stable and Inert  $^{nat}\text{Bi}^{3+}$  and  $^{213}\text{Bi}^{3+}$  Complexation for Potential  $\alpha$ -Radioimmunotherapy Applications. *Chem. Commun.* **2014**, *50*, 12371–12374.

(53) Lima, L. M. P.; Beyler, M.; Delgado, R.; Platas-Iglesias, C.; Tripier, R. Investigating the Complexation of the  $\text{Pb}^{2+}/\text{Bi}^{3+}$  Pair with Dipicolinate Cyclen Ligands. *Inorg. Chem.* **2015**, *54*, 7045–7057.

(54) Wilson, J. J.; Ferrier, M.; Radchenko, V.; Maassen, J. R.; Engle, J. W.; Batista, E. R.; Martin, R. L.; Nortier, F. M.; Fassbender, M. E.; John, K. D.; Birnbaum, E. R. Evaluation of Nitrogen-Rich Macrocyclic Ligands for the Chelation of Therapeutic Bismuth Radioisotopes. *Nucl. Med. Biol.* **2015**, *42*, 428–438.

(55) Egorova, B. V.; Matazova, E. V.; Mitrofanov, A. A.; Aleshin, G. Y.; Trigub, A. L.; Zubenko, A. D.; Fedorova, O. A.; Fedorov, Y. V.; Kalmykov, S. N. Novel Pyridine-Containing Azacrownethers for the Chelation of Therapeutic Bismuth Radioisotopes: Complexation Study, Radiolabeling, Serum Stability and Biodistribution. *Nucl. Med. Biol.* **2018**, *60*, 1–10.

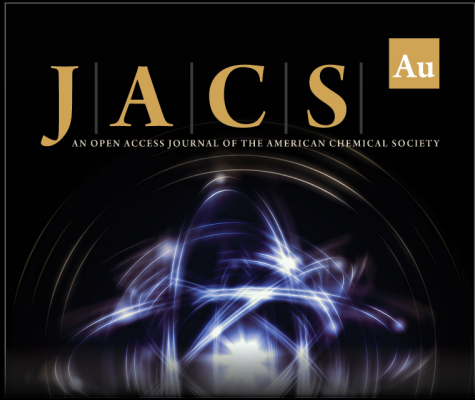
(56) Šimeček, J.; Hermann, P.; Seidl, C.; Bruchertseifer, F.; Morgenstern, A.; Wester, H.-J.; Notni, J. Efficient Formation of Inert Bi-213 Chelates by Tetrakisphosphorus Acid Analogues of DOTA: Towards Improved Alpha-Therapeutics. *EJNMMI Res.* **2018**, *8*, 78.

(57) Matazova, E. V.; Egorova, B. V.; Konopkina, E. A.; Aleshin, G. Y.; Zubenko, A. D.; Mitrofanov, A. A.; Karpov, K. V.; Fedorova, O. A.; Fedorov, Y. V.; Kalmykov, S. N. Benzoazacrown Compound: A Highly Effective Chelator for Therapeutic Bismuth Radioisotopes. *MedChemComm* **2019**, *10*, 1641–1645.

(58) Bruchertseifer, F.; Comba, P.; Martin, B.; Morgenstern, A.; Notni, J.; Starke, M.; Wadepohl, H. First-Generation Bispidine Chelators for  $^{213}\text{Bi}^{\text{III}}$  Radiopharmaceutical Applications. *ChemMedChem* **2020**, *15*, 1591–1600.

(59) Lange, J. L.; Davey, P. R. W. J.; Ma, M. T.; White, J. M.; Morgenstern, A.; Bruchertseifer, F.; Blower, P. J.; Paterson, B. M. An Octadentate Bis(semicarbazone) Macrocyclic: A Potential Chelator for Lead and Bismuth Radiopharmaceuticals. *Dalton Trans.* **2020**, *49*, 14962–14974.

(60) Horváth, D.; Travagin, F.; Guidolin, N.; Buonsanti, F.; Tircsó, G.; Tóth, I.; Bruchertseifer, F.; Morgenstern, A.; Notni, J.; Giovenzana, G. B.; Baranyai, Z. Towards  $^{213}\text{Bi}$  Alpha-Therapeutics and beyond: Unravelling the Foundations of Efficient  $\text{Bi}^{\text{III}}$  Complexation by DOTP. *Inorg. Chem. Front.* **2021**, *8*, 3893–3904.



Editor-in-Chief  
**Prof. Christopher W. Jones**  
Georgia Institute of Technology, USA

**Open for Submissions**

pubs.acs.org/jacsau

ACS Publications  
Most Trusted. Most Cited. Most Read.